Current Pattern Stabilization in Pulsed Plasma Accelerators

A. C. Eckbreth,* K. E. Clark,* and R. G. Jahn†
Princeton University, Princeton, N.J.

Experimental maps of the magnetic field patterns throughout the exhaust plume of a pulsed plasma accelerator driven by a variable length and amplitude rectangular current waveform indicate that the familiar initial process of discrete current sheet propagation is followed by transition to a quasi-steady, more diffuse current conduction pattern. This steady phase, which typically is achieved some tens of microseconds after breakdown, displays essentially unchanged terminal voltage and current characteristics and continues to provide a stream of accelerated gas. The physical details of the transition from propagating to stationary current patterns in a discharge are more conveniently studied in a one-dimensional, parallel-plate configuration, where magnetic probe signatures, Kerr-cell photographs, and terminal voltage measurements again verify the stabilization effect. It is thus suggested that the "snow-plow" sweeping process characteristic of any pulsed plasma accelerator is essentially a starting transient on the steady-flow acceleration mechanism for the same electrode geometry.

I. Introduction

SINCE the early days of electric propulsion, sharp distinction has normally been drawn between steady flow electromagnetic accelerators, such as external crossed-field devices and magnetoplasmadynamic arcs, and unsteady or pulsed electromagnetic accelerators, such as coaxial guns and pinch engines. In the former, one deals with static, diffuse current patterns which interact with external or self-induced magnetic fields to apply a distributed body force to a stream of working fluid passing through the fixed current pattern. In the latter, relatively thin, intense sheets of current are generated which are driven along the accelerator channel by their self-magnetic field, entraining ambient propellant gas as they progress. The typical thruster hardware, terminal power requirements, performance characteristics and limitations, and methods of theoretical analysis of these two classes of accelerator are all substantially different, and their research and engineering development have proceeded largely independently.[1]

In this paper we describe a series of basic experiments that indicate that this rigid separation of steady flow and pulsed plasma acceleration may be artificial. Specifically, it is observed that spontaneous transition from a pulsed mode to a steady mode can be achieved in various accelerator geometries, with minimal effect on the terminal characteristics of the device, including the ejected propellant stream. To this extent it appears that the pulsed plasma acceleration process is simply an initiation phase, or "switching transient," on the steady process eventually established in a given electrode geometry and that much of the microscopic scale acceleration and current conduction mechanisms are common to both phases.

II. Exhaust Plume Studies

The first indication of spontaneous transition from a pulsed to a steady acceleration mode was observed when a series of pulsed pinch exhaust plume studies reported previously[2] were extended to allow much longer driving current waveforms. These experiments were performed using a 5-in.-diam × 2-in.-length linear pinch discharge in argon as a source of plasma to be ejected through a large axial orifice, as shown in Fig. 1. The outer surface of the anode of the discharge chamber extends to a 34-in. diam and contains a 4-in.-diam orifice which opens into a large Plexiglas vacuum tank. This 3-ft-diam × 4-ft-long tank, described in detail elsewhere,[3] was constructed to provide an environment for development of the exhaust plume as free as possible from spurious electrostatic, electromagnetic, and gasdynamic interactions with the tank walls. In the experiments to be described, the ambient pressure in the tank, when not purposely set to some higher value, could be maintained below 0.05 μ, where the mean free path exceeded tank dimensions.

The discharge is driven by a bank of 40 × 3.2-μf capacitors divided into four individual lines composed of ten capacitors and ten inductors in the form of an LC ladder network. Each individual line can produce a pulse of roughly 30,000 amp × 20 μsec when charged to 10,000 v. Connecting the four banks in parallel provides a pulse of 120,000 amp × 20 μsec. Series connection produces a 30,000-amp × 80-μsec pulse. Figure 2 shows a Rogowski coil record of a typical waveform delivered to the discharge. In each case,

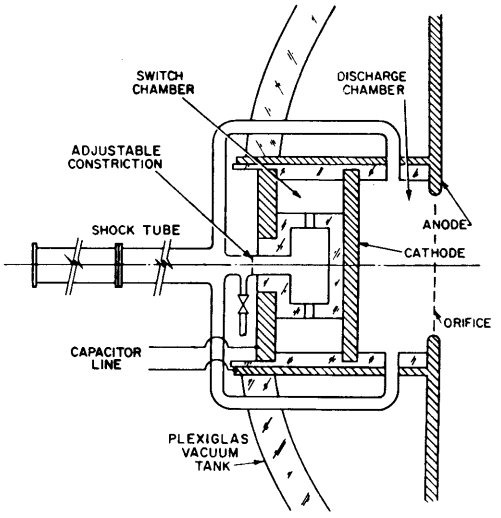

Fig. 1 Cross section of plasma pinch-orifice device (schematic).

Presented as Paper 67-656 at the AIAA Electric Propulsion and Plasmadynamics Conference, Colorado Springs, Colo., September 11–13, 1967; submitted November 3, 1967; revision received June 13, 1968. This program is supported by NASA Grant NGR-31-001-005.

* Graduate Student, Guggenheim Laboratories, Department of Aerospace and Mechanical Sciences. Student Member AIAA.

† Professor of Aerospace Sciences, Guggenheim Laboratories, Department of Aerospace and Mechanical Sciences. Associate Fellow AIAA.

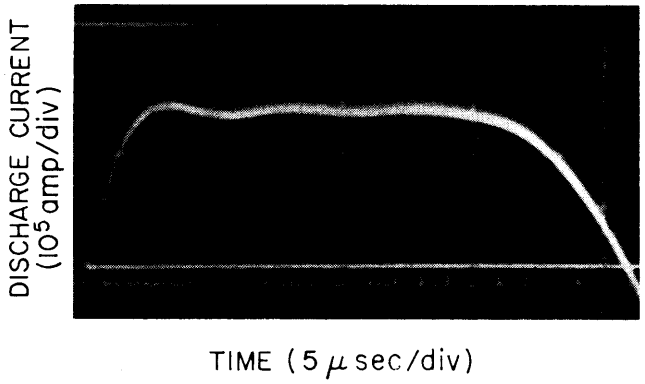

Fig. 2 Typical discharge current waveform.

the bank is switched across the chamber electrodes by a gas-triggered pinch discharge switch mounted adjacent to the cathode and coaxial with the main chamber.[4]

To explore the effect of back pressure on development of the exhaust plume, two extreme cases were studied. In one, the "ambient" mode, both the exhaust vessel and pinch chamber are simply preset with argon at 100 μ. In the other, the pinch chamber and vacuum vessel are both evacuated below 0.05 μ and the discharge process is initiated by gas injection from a shock tube source which simultaneously supplies both the switch and pinch chambers. As shown schematically in Fig. 1, a variable diameter orifice in the switch supply line permits correlation of the chamber filling cycle with the time of discharge initiation. In practice, the average pinch chamber pressure at breakdown is inferred by matching photographically observed pinch times with those of the ambient mode at the corresponding pressure. It may reasonably be questioned whether such a gas injection procedure sensibly raises the pressure throughout the environmental tank before the discharge occurs. To check this, time-resolved pressure measurements were obtained in the exhaust region with a fast-response, miniature ionization gage.[5] Figure 3 displays the axial pressure profile at the instant when the chamber reaches the desired discharge pressure of 100 μ. It is seen that this axial decay is sufficiently rapid that no sensible increase from the preset back pressure is felt further than some three orifice diameters from the anode. Since the radial decay is found to be of the same magnitude, it can be safely assumed that the finite dimensions of the exhaust tank do not interfere with the plume development.

The principle diagnostic tool employed is a four-element rake of magnetic probes, whose signals are passively integrated on the scope to yield simultaneous records of local magnetic field B_θ vs time at four positions in the plume.

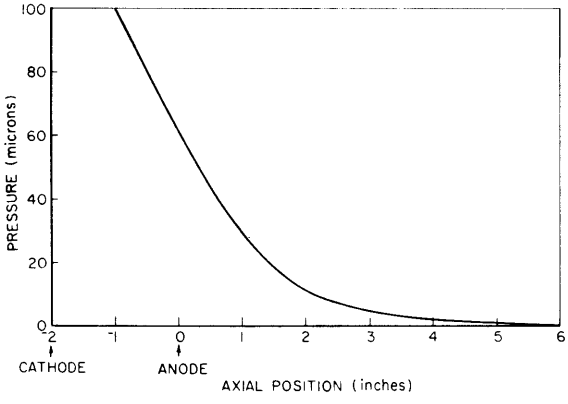

Fig. 3 Axial pressure profile from shock tube injection at time of discharge.

In addition, straight and bent probes are inserted through the sidewalls of the pinch chamber to study its interior processes. Application of Ampere's law to each probe record yields the total current enclosed in a circular area whose radius is that of the probe position and whose center lies on the chamber axis. The data may thus be plotted in the form of contours of enclosed current in the r, z plane at successive times.

Figure 4 shows a series of such enclosed current contours for the 30,000-amp $\times$ 80-μsec discharge in 100-μ ambient argon, computed from triple-overlay probe records judiciously averaged over the demonstrated reproducibility of the pattern ($\sim \pm 10\%$). The major effect to be noted is that the initial unsteady process of discrete current sheet propagation is followed by transition to a stable, diffused current pattern. This stabilization may also be displayed as plots of maximum axial and radial progression of the enclosed current contours, as shown in Fig. 5. It is apparent from these figures that stabilization occurs approximately midway through the pulse.

Figure 6 shows the sequence of patterns of enclosed current found for the same discharge current waveform when the shock tube injection system is employed. The anticipated quantitative differences in contour location caused by the steep density profiles awaiting the discharge are evident, but once again a cessation of contour propagation occurs about midway through the pulse. Results of the high-current (120,000 amp $\times$ 20 μsec) pulse are less conclusive in that, although propagation of the contours noticeably slows, full stabilization is not achieved. Presumably the pulse length available at this current level is insufficient to allow completion of the transition. A full display of all measured contours is available.[6]

Following these first evidences of the transition phenomena, a series of crude experiments were performed with ion-collecting probes and terminal voltage dividers to verify that in their stabilized phase the discharges continue to accelerate gas. Rather than reviewing these results, a sequence of more controlled experiments in a simpler geometry which bear on the same point will be discussed in the following section.

The preliminary experiments described previously suggest two avenues of detailed study. On the one hand, there is an interest in precise interior examination of the physics of the process of spontaneous transition from a propagating, "sweeping" discharge configuration, to a quasi-steady, "blowing" configuration. On the other hand, there now opens the possibility of quasi-steady simulation of various steady flow accelerators of propulsion interest, such as the magnetoplasmadynamic arcs. For neither purpose is the electrode geometry of the aforementioned experiments optimum. The remainder of this paper describes a series of experiments in a parallel-plate accelerator to study the transition process in more detail. A subsequent paper discusses the development of a suitable quasi-steady magnetoplasmadynamic simulator and the results therefrom.

III. Parallel-Plate Accelerator

The phenomenological observations of the stabilization process in the exhaust plumes described previously do not permit conclusive assignment of the essential cause of this transition, nor indicate its scaling properties. One may reasonably speculate that it is basically a geometrical effect, associated with the finite electrode dimensions and the corresponding limiting configuration to which the current pattern can expand before its driving mechanism fails. But whether this failure is an inability of the available interelectrode potential to sustain an arc column of greater length or a weakening of the local $\mathbf{j} \times \mathbf{B}$ force density to the point that the plume can no longer sensibly progress against the ambient gas is not clear. Also unclear is the role of the

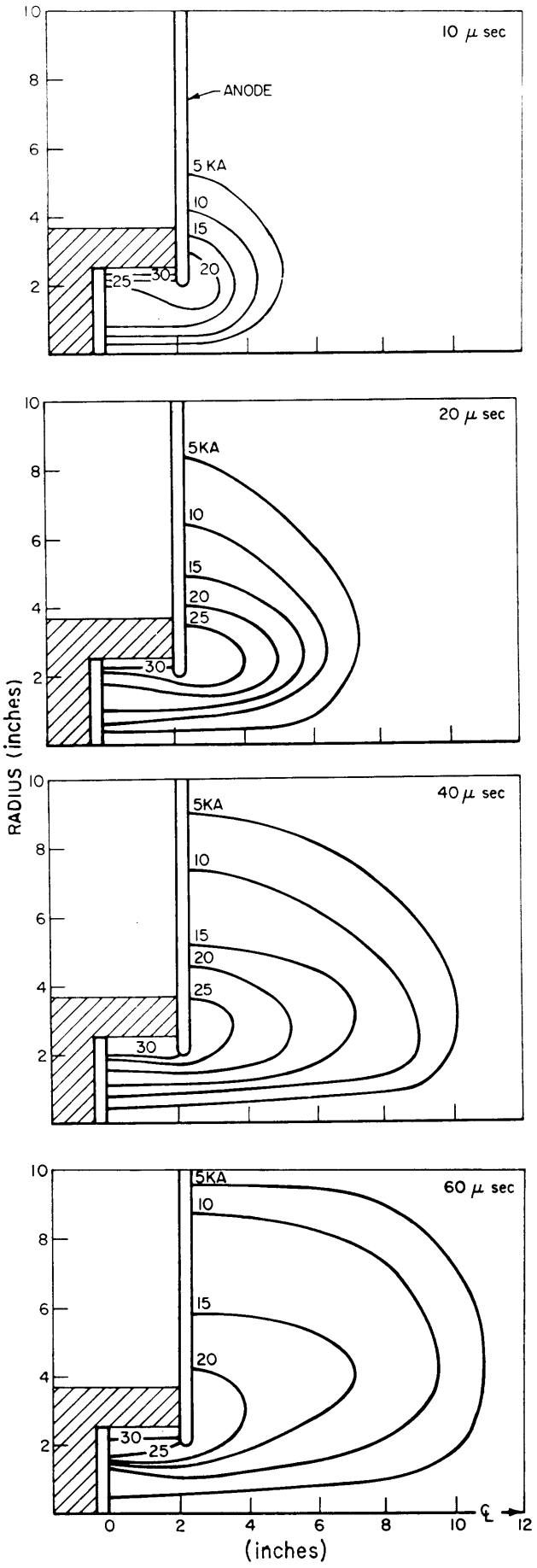

Fig. 4 Enclosed current contours in exhaust plume of 30,000-amp × 80-μsec discharge in 100-μ ambient argon.

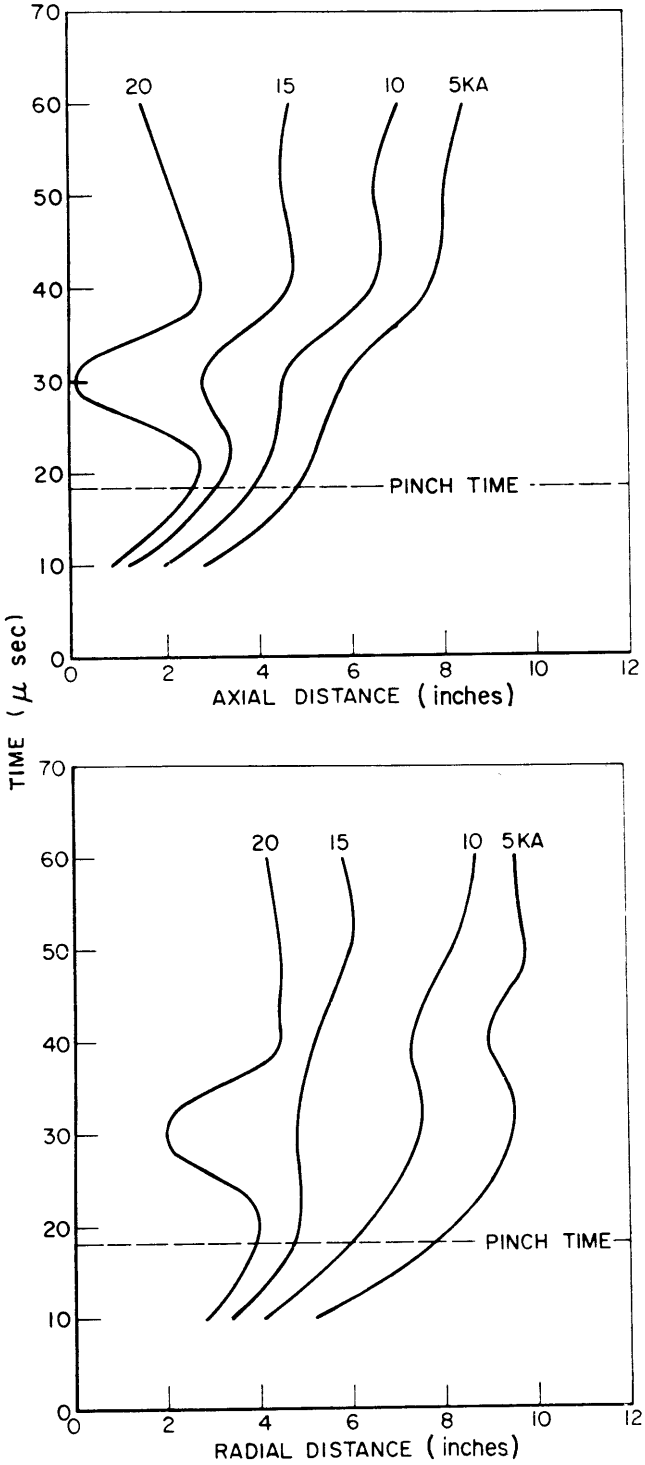

Fig. 5 Maximum axial and radial progression of enclosed current contours in exhaust plume of 30,000-amp × 80-μsec discharge in 100-μ ambient argon.

ambient density profile which is observed to modify, but not to inhibit, the stabilization process.

In an effort to separate the effect of these various influences and to study the interior details of stabilizing discharge patterns in a simpler geometry, a parallel-plate accelerator[7,8] was constructed to operate over a range of dimensions, current and gas densities, and driving current waveforms comparable to those of the exhaust orifice device studied earlier. This accelerator, sketched in Fig. 7, is essentially a rectangular box with metal electrodes on top and bottom and four insulator sidewalls, formed by boring out one solid piece of Plexiglas. The interior dimensions of the channel are 48-in.

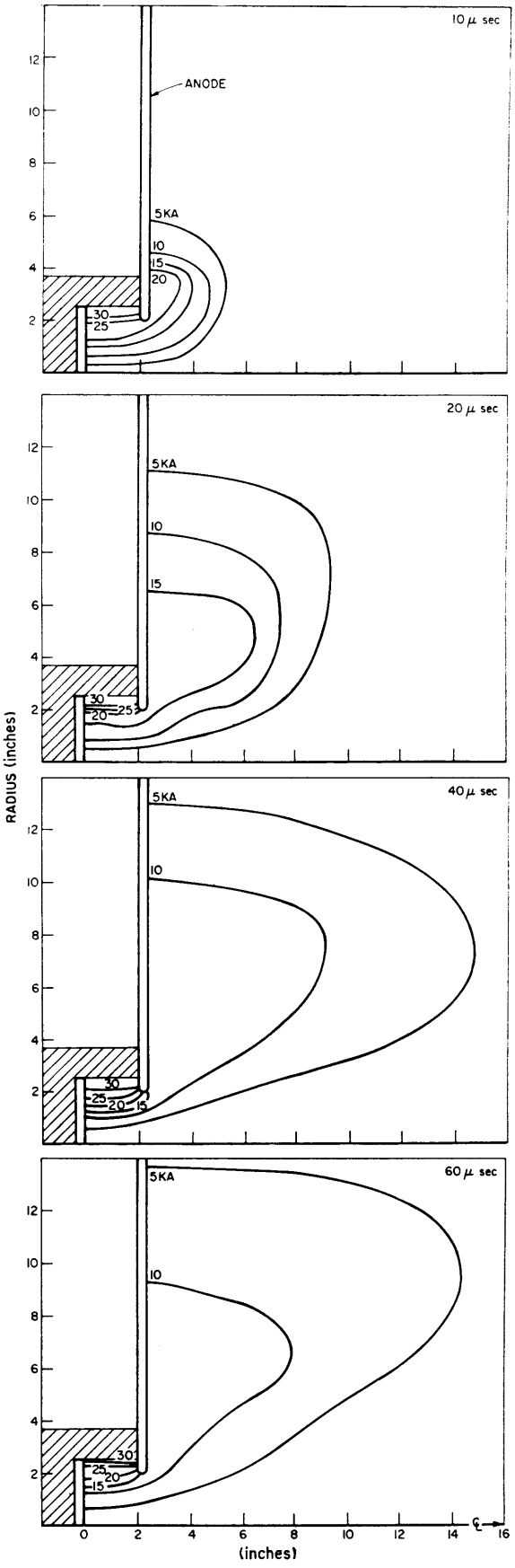

Fig. 6 Enclosed current contours in exhaust plume of 30,000-amp × 80-μsec discharge, shock tube injection.

length, 6-in. width, and 2-in. interelectrode gap. The full electrode length will accommodate the anticipated maximum excursion of a propagating current sheet driven by the available capacitor bank, but, for systematic study of the stabilization event, it is possible to cover portions of the electrodes with insulating material, as described below. The electrode width is selected as a compromise between minimizing edge effects on the current sheet and maintaining adequate current density for effective gas entrainment, based on experience with other discharge geometries. The electrode gap conforms to the bulk of the earlier work with linear pinch configurations.

In typical operation, the upper electrode is the anode and is connected at one end to the capacitor pulse line and at the other to a ground plane leading to the diagnostic screen room. The lower electrode connects to the negative side of the line through a gas discharge switch mounted directly beneath the channel. A 1000 Ω ballast resistor holds both electrodes at ground potential during charging of the line to 10,000 v. The switch is then discharged with a puff of argon, transferring the voltage to the main chamber electrodes, thereby initiating a current sheet across the channel at the line end. For the experiments described below, the channel is initially pumped to 0.5 μ and then filled with argon to 100 μ. A pulse line similar to that described previously is connected to deliver either a nominal 120,000-amp × 20-μsec pulse or a 30,000-amp × 80-μsec pulse.

Prior to searching for a current sheet stabilization condition, the characteristics of this geometry in the conventional unsteady, or propagating sheet mode were assessed using the full metal electrode arrangement described previously. A sequence of Kerr-cell photographs and magnetic probe measurements indicate no tendency of the sheet to slow its propagation throughout the duration of the pulse. These do, however, reveal certain unexpectedly severe two-dimensional distortions of the current sheet geometry. Figure 8 displays a series of typical Kerr-cell photographs obtained with the camera looking through the Plexiglas sidewall, normal to the direction of propagation at a succession of adjacent positions between the bolts, to follow the progress of the luminous sheet. Note the development of a diffuse "anode foot" which enlarges and grows as the sheet propagates down the channel. Inception of such a foot has been observed in other experiments of this type,[9,10] but here it has been allowed to progress to the point where it completely dominates the entire luminous pattern, tilting it substantially with respect to the axis, and diffusing it over a large dimension. From a similar series of photographs taken at a perspective angle, however, the process is observed to remain two-dimensional, stretching from sidewall to sidewall across the electrodes. Because of the tilting and diffusing of the luminous pattern, it is difficult to define a mean trajectory precisely, but, to a crude estimate, the propagation speeds are in the range of 40,000 m/sec for the 120,000-amp × 20-μsec pulse and 20,000 m/sec for the 30,000-amp × 80-μsec pulse.

The qualitative aspects of the luminous photographs are confirmed by magnetic probe data obtained in the conventional manner. The probes employed are Formvar wire coils epoxyed into sealed Pyrex tubes and inserted through access ports drilled in the anode. The signals are passively integrated at the scope face to provide records of magnetic field vs time at selected channel positions, which then can be translated into spatial distributions of current density. These patterns are found to be quite reproducible and nearly two-dimensional over the bulk of the channel width. Typical

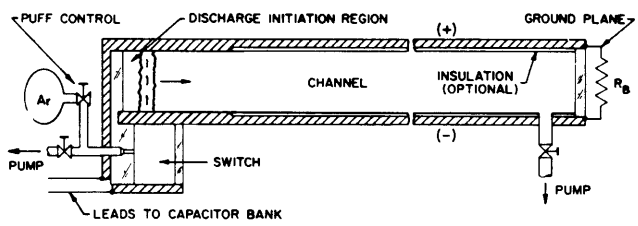

Fig. 7 Parallel-plate accelerator (schematic).

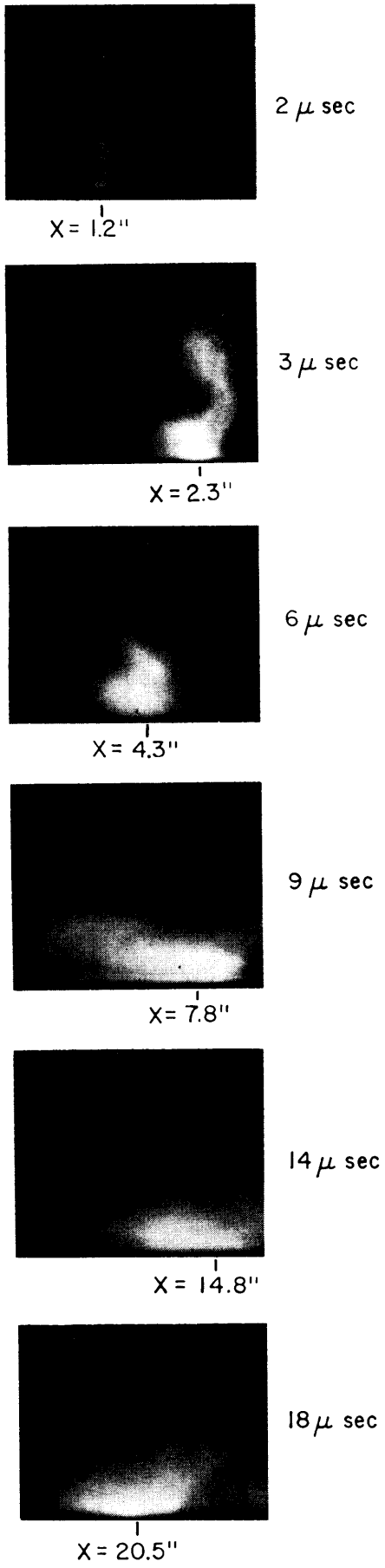

Fig. 8 Kerr-cell photographs of propagation of luminous front in parallel-plate accelerator at various positions X downstream of initiation location: 120,000-amp × 20-μsec driving current, 100-μ argon, full electrodes.

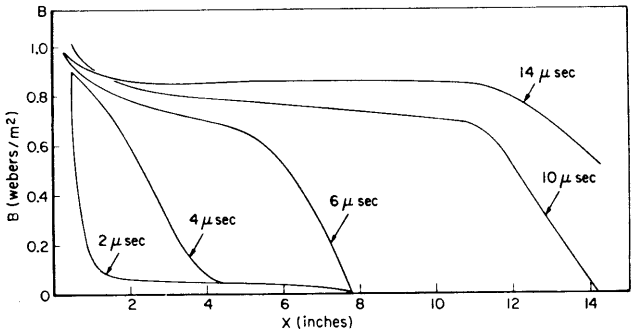

Fig. 9 Magnetic field amplitude along parallel-plate accelerator: 120,000-amp × 20-μsec driving current, 100-μ argon, full electrodes.

profiles of magnetic field vs axial distance along the midline of the channel at various times are shown in Fig. 9. The corresponding current density patterns, which are essentially the spatial derivatives of the magnetic field profiles, tend to be sharply peaked at the outset and then to broaden as they propagate down the channel at roughly the velocities quoted previously for the luminous fronts.

In an attempt to stop the propagation of the current sheet and precipitate transition to the steady mode of acceleration, the channel was modified in the following fashion: both electrode surfaces were covered with 0.003-in. Mylar sheet insulation from a position $9\frac{1}{2}$ in. downstream of the discharge initiation location, to the far end of the channel (Fig. 7), so that the propagating discharge, upon reaching the end of the conducting surface, would be forced either to extend its length further and further while its ends remained attached to the last edges of the conductors or to lapse into a stationary pattern near the discontinuity. In all cases studied, the discharge elected the latter mode.

Using this arrangement, Kerr-cell, magnetic probe, and voltage divider studies were repeated for otherwise identical conditions to those described previously, and, by comparison of the results for the full electrode and partial electrode situations, transition of the current zone to a steady mode was clearly established. For example, Fig. 10 shows a sequence of luminous photographs taken slightly downstream of the electrode discontinuity. Note that now when the propagating luminous front reaches the end of its exposed electrode, it essentially stops and changes its character drastically, eventually settling into two horizontal bands, near the (covered) anode and cathode surfaces, respectively, with a darker region in the midplane of the gap. One may speculate that these bright bands are analogous to the anode and cathode jets commonly seen in the magnetoplasmadynamic arcs. Figure 11 summarizes the comparison of luminous front propagation in the various full electrode and partially insulated electrode cases studied.

Confirmation that the current-carrying region has indeed ceased to propagate is best supplied by maps of enclosed current contours derived from magnetic probing of the entire discharge volume. Figure 12 displays such contours for the two driving current waveforms studied. In these sketches, the individual contours conform to local current streamlines, and their numeral indicates the cumulative current passing everywhere upstream. For the high current pulse (part a), the major current zone proceeds directly to a pseudo-steady pattern which is somewhat bowed downstream, but at no time projects more than 6 in. beyond the discontinuity. In the low current case (part b), the current zone first overshoots somewhat (dotted contours), then springs back to a flatter pseudo-steady pattern (solid contours).

Additional confirmation of the stabilization of the current pattern and valuable indication that the pattern indeed

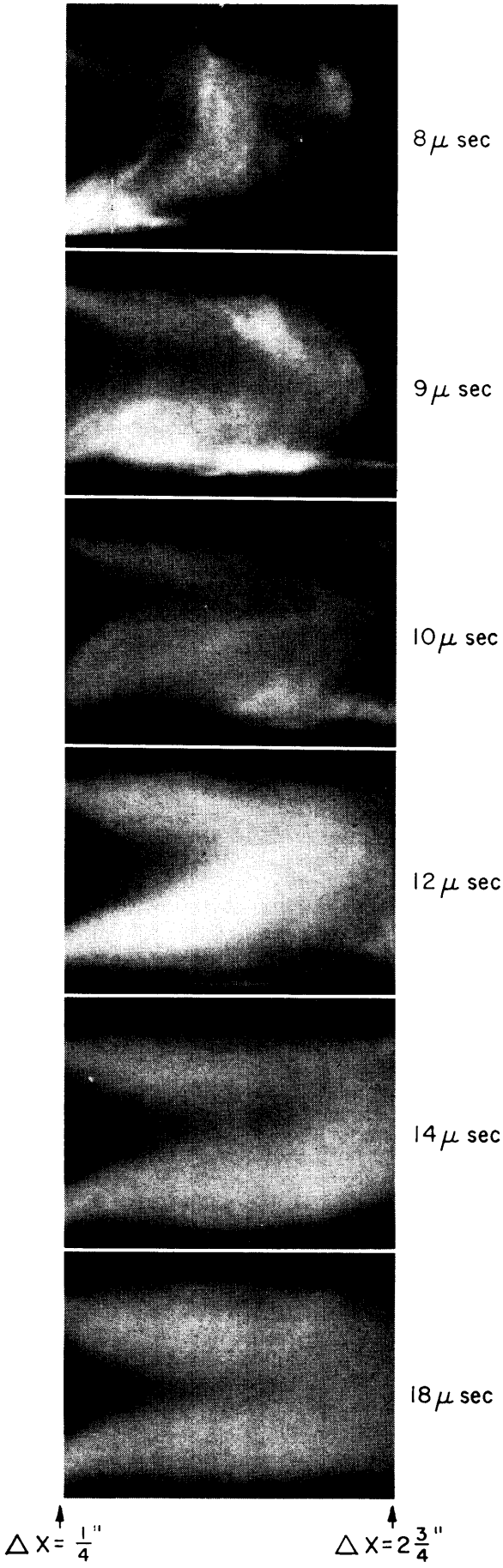

Fig. 10 Kerr-cell photographs of development of discharge luminosity pattern downstream of electrode discontinuity ($\Delta X \equiv 0$): 120,000-amp × 20-μsec driving current, 100-μ argon, partially insulated electrodes.

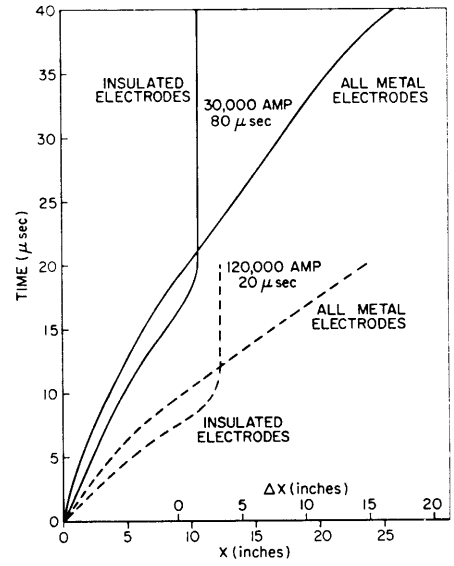

Fig. 11 Trajectories of luminous fronts in parallel-plate accelerator.

continues to accelerate gas through itself in its stabilized phase is provided by a sequence of terminal voltage measurements with an inner divider. This device is simply a voltage tap that passes through an insulated port in the anode to electrical contact with the cathode and enables one to separate the resistive and inductive voltage drops in the plasma (Fig. 13). At any given position along the channel A, the inner divider first records only the resistive voltage drop through the plasma current sheet. If and when the current sheet sweeps by the probe position B, it then records an additional voltage corresponding to the increase in magnetic flux linked by the probe circuit. For constant driving current and a sharply defined current sheet, this flux increase is simply proportional to sheet speed. Finally, if the current sheet should come to rest and start accelerating gas through itself, the probe also records the corresponding motional emf, regardless of its location relative to the sheet. Figure 14 presents voltage signals from probes of this type which display each of these three contributions. In Fig. 14a we see the response of a probe located about 8 in. downstream of the initial breakdown location in the full-electrode accelerator. Following a short burst of initiation noise, the probe first records a resistive drop of about 60 v for about 3 μsec (corresponding to a total plasma resistance of about 0.0005 ohm); as the current sheet sweeps by, the inductive contribution is added to the voltage, bringing it to some 700 v, where it remains relatively constant for the duration of the driving current waveform, corresponding to a constant speed propagation of the sheet far down the channel. In contrast, Fig. 14b shows the response of a probe located far enough

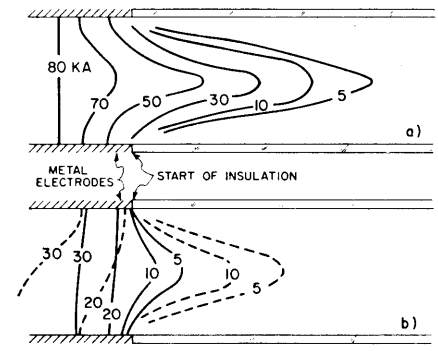

Fig. 12 Enclosed current contours for stabilized phase of parallel-plate accelerator; 100-μ argon: a) 120,000-amp × 20-μsec driving current; b) 30,000-amp × 80-μsec.

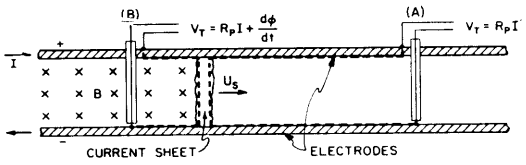

Fig. 13 Inner divider at two locations in parallel-plate accelerator (schematic).

from the breakdown location that the sheet does not reach it during the lifetime of the pulse. Here we see (on an amplified scale) the resistive drop alone over the full time of the pulse.

The aforementioned experiments are now repeated using the partially insulated electrodes described earlier. Curiously, the response of the probe 8 in. from the initiation position (Fig. 14c) is almost identical to that for the full electrode case (14a), despite the fact that the current sheet stabilizes at the discontinuity some 10 μsec into the pulse, thereby eliminating the flux increase contribution. One hypothesis is that the stabilization process is accompanied by an onset of gas pumping through the sheet of just the right magnitude to provide a motional or back emf equal to the lost inductive contribution. However, if this is the case, the motional emf component must also appear on the probe far downstream, since, in a truly steady process, the voltage drop between electrodes should be the same everywhere along the channel. Indeed, referring to Fig. 14d, we see that, unlike the corresponding signal in the full electrode case (Fig. 14b), the resistive contribution is supplemented by the motional emf at the time of sheet stabilization, bringing this voltage just to the value of the upstream divider (Fig. 14c). It thus appears that we are here observing a new and rather powerful electromagnetic inertial mechanism; i.e., when the motion of the conducting current sheet is arrested at the electrode discontinuity, the back emf generated in opposition to this change is just sufficient to maintain the terminal voltage at its previous level. The impressive feature of this effect is that the gasdynamic processes involved in its accomplishment are fundamentally quite distinct. That is, there has been a transition from the familiar unsteady mode of gas accumulation in a propagating current sheet, to the equally familiar but rather different steady mode of gas "blowing" through a fixed current pattern, with no observable change in terminal voltage.

As still another demonstration of the effective gas acceleration provided by the stabilized current patterns in the insulated electrode channel, a simple double wedge "airfoil" of 15° half-angle was positioned in the channel at various

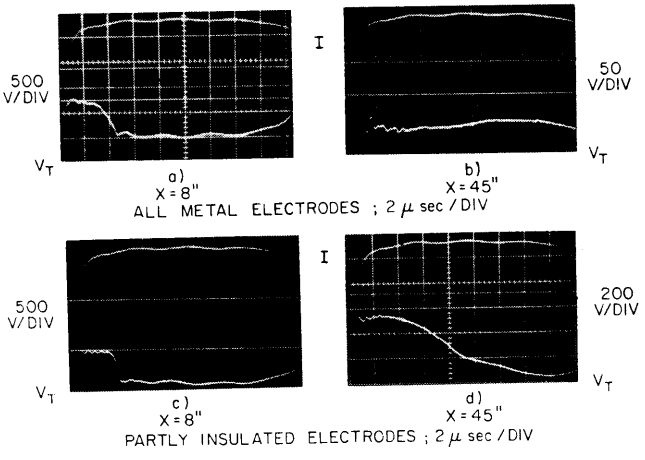

Fig. 14 Comparison of inner divider responses in parallel-plate accelerator at two positions X downstream of initiation location; 100-μ argon; 120,000-amp × 20-μsec driving current.

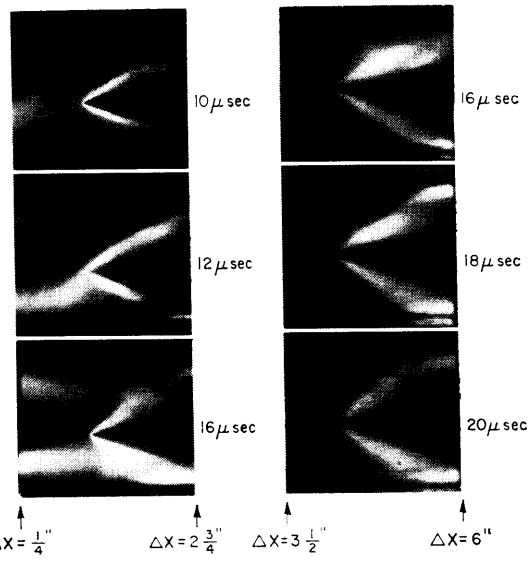

Fig. 15 Kerr-cell photographs of flow over wedge in parallel-plate accelerator with partially insulated electrodes; 100-μ argon; 120,000-amp × 20-μsec driving current.

locations downstream of the electrode discontinuity. Figure 15 shows Kerr-cell photographs of the resulting luminous patterns of the flow for the 120,000-amp × 20-μsec pulse, taken at locations some 2 and 5 in. downstream of the electrode discontinuity. At the first position, where there is considerable discharge current bowing downstream, one first sees a transient surge of snowplowed gas sweep by the wedge followed by development of a steady flow which produces attached oblique shocks. At the 5-in. position, which is reached by very little discharge current, oblique shocks are again visible on the wedge at the later times after stabilization has occurred. Thus, we must conclude that substantial gas flow exists both within and downstream of the stabilized current pattern over the lifetime of the driving pulse, even though the ambient gas pressure downstream is very high and even though there is no evident source of gas provided upstream of the acceleration region.

In an effort to unravel a bit more of the mechanisms of gas acceleration in the two phases, attempts have been made to map the patterns of streamwise electric field within the current-carrying regions of the plasma with a coaxial double probe.[11] The probe response along the metal electrode portion of the channel corresponds to that commonly observed for a propagating current sheet, namely, a "spike" of forward-facing electric field, followed by a weaker region of field reversal. In contrast, probe signatures obtained within the stabilized current distribution, downstream of the metal-to-insulation junction, consist of a vestige of the current sheet spike, followed by a null period, followed by a step function increase lasting until the end of the pulse (Fig. 16).

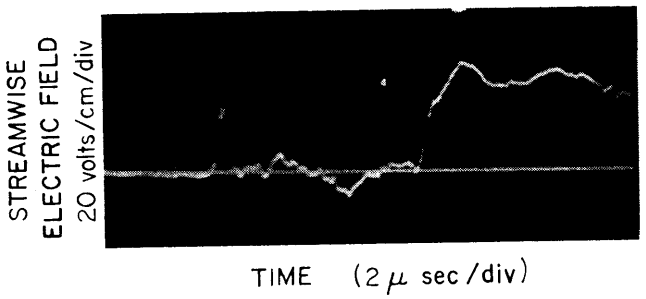

Fig. 16 Streamwise electric field in parallel-plate accelerator, 3.8 in. downstream of electrode discontinuity; 100-μ argon; 120,000-amp × 20-μsec. driving current.

The amplitudes of the vestigial spike and of the plateau decrease with distance downstream of the electrode discontinuity. The former decelerates perceptively once past the discontinuity, but the leading edge of the plateau seems to maintain a uniform speed or even to accelerate somewhat.

One may speculate that the first spike recorded by the probe announces the arrival of the snowplowed plasma accumulated by the propagating sheet upstream in the conducting portion of the channel, now continuing on its own inertia as the sheet is arrested near the discontinuity and diffuses into the quasi-steady conduction pattern. The plateau of electric field prevailing over the latter portion of the response presumably reflects the quasi-steady flow acceleration process in operation, possibly as a Hall voltage component of the total electric field. The rather well-defined null time between these two signals is somewhat puzzling, particularly since no correspondingly abrupt processes are evident in the development of the discharge current distribution in this region.

IV. Discussion

One reasonable question to be raised in the interpretation of the alleged transition to quasi-steady acceleration described previously is the source of mass flow to the stabilized current zone. If, in the transient phase, the propagating current sheet completely sweeps out the ambient fill of gas, none would remain for later ingestion into the blowing acceleration zone, yet the experiments indicate a persistence of accelerated outflow from this zone over the entire driving current pulse duration. Three possibilities may be considered: 1) the propagating current sheet is semipermeable and leaves behind a residue of partially accelerated gas which later provides the inflow to the stabilized current zone, 2) the stationary discharge ablates electrode material, or 3) the stationary discharge ablates insulator material, which it then accelerates. If alternative 1 dominates, it can persist for only a limited period before exhausting this mass supply, so that for longer pulses the outflow should decay at later times, and this tendency is indeed observed for the 30,000-amp $\times$ 80-μsec pulse.

If the quasi-steady discharge is starved for inlet mass flow, one may expect some differences in its behavior when provision for an external supply of gas is made. To make such comparison, a shock-tube gas injection system similar to that described in Sec. II has been installed on the parallel-plate accelerator. However, the voltage signatures and wedge flow photographs for the two current waveforms show no convincing differences between 100-μ ambient fill and shock-tube injection set to provide 100-μ channel pressure at breakdown. In retrospect, this now seems reasonable, since the available time scale is probably too short for the injection flow to become properly established. In essence, the injected flow has the task of filling the channel void created by the sweeping current sheet as it propagates to its stabilized position. This filling process must require a time of the order of the channel length involved, divided by the sound speed of the injected gas, i.e., hundreds of microseconds. In other words, although it appears that the electrodynamic aspects of steady plasma acceleration can be simulated on a time scale of tens of microseconds, attainment of the corresponding quasi-steady gas flow from an external reservoir to the final accelerated stream will require an order of magnitude longer test time. Experiments extending the techniques described previously to this longer time scale are currently in progress.

Also in progress is a complementary program of experiments to exploit the stabilization phenomenon in a coaxial electrode geometry replicating the steady magnetoplasmadynamic arc, for purposes of extending study of that device into ranges of power density inaccessible to ground-based steady flow facilities.

References

[1] Jahn, R. G., *Physics of Electric Propulsion*, McGraw-Hill, New York, 1968.

[2] Jahn, R. G., von Jaskowsky, W., and Burton, R. L., "Ejection of a Pinched Plasma From an Axial Orifice," *AIAA Journal*, Vol. 3, No. 10, Oct. 1965, pp. 1862–1866.

[3] Jahn, R. G. and Clark, K. E., "A Large Dielectric Vacuum Facility," *AIAA Journal*, Vol. 4, No. 6, June 1966, p. 1135.

[4] Jahn, R. G., von Jaskowsky, W., and Casini, A. L., "Gas-triggered Pinch Discharge Switch," *The Review of Scientific Instruments*, Vol. 36, No. 1, Jan. 1965, pp. 101–102.

[5] Valsamakis, E. A., "Ionization Gauge for Transient Gas Pressure Measurements," *The Review of Scientific Instruments*, Vol. 37, No. 10, Oct. 1966, pp. 1318–1320.

[6] Jahn, R. G. and von Jaskowsky, W., "Pulsed Electromagnetic Gas Acceleration," AMS TR-634h, Jan. 1967, Dept. of Aerospace and Mechanical Sciences, Princeton Univ., Princeton, N.J.

[7] Lovberg, R. H., "Acceleration of Plasma by Displacement Currents Resulting From Ionization," *Proceedings of the Sixth International Conference on Ionization Phenomena in Gases*, Paper IX, 6, 1963, pp. 235–239.

[8] Maes, M. E., "Experimental Investigation of the Confined Parallel Rail Pulsed Plasma Accelerator," *Proceedings of Third Annual Symposium on Engineering Aspects of Magnetohydrodynamics*, edited by N. W. Mather and G. W. Sutton, Gordon & Breach, New York, 1964, pp. 439–465.

[9] MacLelland, J. R., MacKenzie, A. S., and Irving, J., "Schlieren Photography of Rail Tube Plasmas," *The Physics of Fluids*, Vol. 9, No. 8, Aug. 1966, p. 1613.

[10] Liebing, L., "Motion and Structure of a Plasma Produced in a Rail Spark Gap," *The Physics of Fluids*, Vol. 6, No. 7, July 1963, pp. 1035–1036.

[11] Burkhardt, L. C. and Lovberg, R. H., "Current Sheet in a Coaxial Plasma Gun," *The Physics of Fluids*, Vol. 5, No. 3, March 1962, pp. 341–347.